Luminescence of *N*-Arylbenzamides in Low-Temperature Glasses

Frederick D. Lewis* and Weizhong Liu

Department of Chemistry, Northwestern University, Evanston, Illinois 60208-3113

Received: August 2, 1999; In Final Form: October 1, 1999

The low-temperature luminescence of benzamide and six additional *N*-arylbenzamides has been investigated in a methyltetrahydrofuran glass. The luminescence of microcrystalline benzamide has also been studied. Assignments of the fluorescence and phosphorescence have been made on the basis of comparisons with the spectra of benzamide and the six aminoarenes and with the results of semiempirical ZINDO calculations for the amines and amides. This information was used to construct state-energy diagrams for the six amides. The 430 nm fluorescence of benzanilide and the amides derived from 4-aminobiphenyl and 4-aminodiphenylacetylene is assigned to a n,π^* state having a relaxed geometry and localized on the benzoyl group. The structured fluorescence of the amides derived from 4-aminostilbene and 2-aminoanthracene is attributed to a delocalized π,π^* singlet state. The amide derived from 2-aminophenanthrene displays dual fluorescence. The amides derived from 4-aminostilbene and 2-aminoanthracene are nonphosphorescent. The structured phosphorescence of the amides derived from the other aminoarenes is assigned to a π,π^* triplet state similar to that for the aminoarene. These results serve to further elucidate the unusual luminescence properties of the benzamides in solution as well as in low-temperature glasses.

Introduction

Benzanilide (**1**) displays broad, weak, Stokes-shifted fluorescence in nonpolar solvents at room temperature.[1−5] Its absorption and emission maxima in methylcyclohexane solution are at 265 and 475 nm, respectively, and its fluorescence quantum yield is 0.6×10^{-3}.[5] This emission has been attributed variously to an imidol tautomer, to a TICT state whose formation requires twisting about the amide C−N bond, and to dual emission from both a tautomer and TICT state.[6] Stokes-shifted fluorescence is not observed in model compounds that cannot undergo C−N rotation.[2] A second, weaker fluorescence has also been observed in nonpolar solvents and variously attributed to a Franck−Condon singlet state or to a fluorescent impurity.[2,5]

Intense luminescence with a maximum of ca. 430 nm is observed in both nonpolar and polar glasses at 77 K.[4,7] Luminescence with a maximum at 410 nm is also observed from crystalline benzanilide.[2] The luminescence in glasses is attributed to overlapping fluorescence and phosphorescence, with the fluorescence maximum occurring at a longer wavelength than the phosphorescence maximum (430 vs 410 nm). The low-temperature fluorescence has been attributed to an n,π^* singlet state localized on the benzoyl group;[4] however, the nature of the lowest triplet state has not been determined. Thus, no explanation exists for the peculiar inversion of fluorescence and phosphorescence maxima.

Our interest in the photophysics and photochemistry of aromatic amides[5,8,9] led us to investigate a family of six *N*-arylbenzamides (Chart 1) in which the size of the *N*-aryl group is increased from aniline to 2-aminoanthracene. By lowering the singlet and triplet energy of the *N*-aryl group, we hoped to determine whether the singlet and triplet states of benzamides are delocalized or whether they are localized on the benzoyl and aminoarene subunits. Studies of luminescence in low-temperature glasses offers several advantages over solution studies; namely, restricted molecular motion, more intense fluorescence, and the observation of phosphorescence as well as fluorescence. Comparative analysis of the fluorescence and phosphorescence of the six *N*-arylbenzamides with those of benzamide and the primary aminoarenes was used in conjunction with semiempirical ZINDO calculations to construct state-energy diagrams. The fluorescence of benzanilide and the amides derived from the smaller aminoarenes is assigned to an n,π^* state having a relaxed geometry localized on the benzoyl group, whereas the amides derived from the larger amines display fluorescence from a delocalized π,π^* singlet state. In all cases where phosphorescence is observed, it arises from a π,π^* triplet state similar to that for the aminoarene. These results serve to further elucidate the unusual luminescence properties of the benzamides in solution as well as in low-temperature glasses.

CHART 1

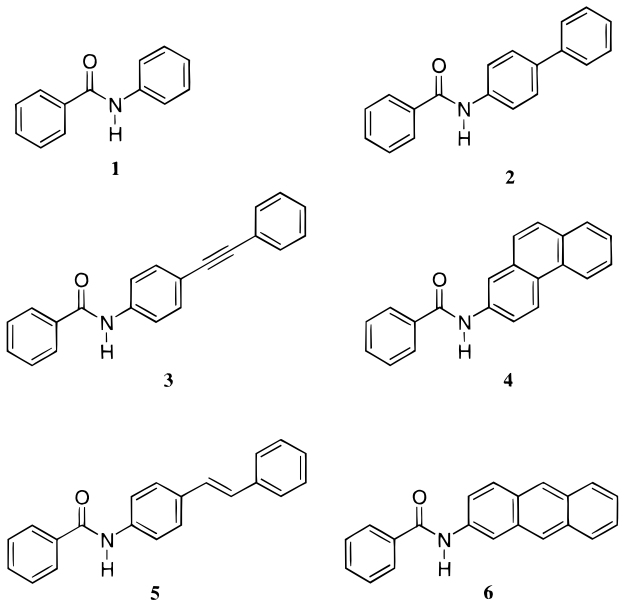

* Corresponding author. E-mail: lewis@chem.nwu.edu.

10.1021/jp9927294 CCC: $18.00
Published on Web 11/05/1999

further elucidate the unusual luminescence properties of the benzamides in solution as well as in low-temperature glasses.

Experimental Section

General Methods. ^{1}H NMR spectra were measured on a Varian Gemini 300 spectrometer. UV−vis spectra were measured on a Hewlett-Packard 8452A diode array spectrometer using a 1 cm path length quartz cell. Total emission spectra were measured on a SPEX Fluoromax spectrometer. Low-temperature spectra were measured either in a Suprasil quartz EPR tube (i.d. = 3.3 mm) using a quartz liquid nitrogen coldfinger dewar at 77 K or in an Oxford Cryogenics DN1704 cryostat fitted with a Oxford Instruments ITC4 temperature controller. Total emission quantum yields were measured by comparing the integrated area under the total emission curve at an equal absorbency and the same excitation wavelength as an external standard, 9,10-diphenylanthracene ($\Phi_f \sim 1.0$ at 77 K in methyltetrahydrofuran (MTHF)).[10] In the case of aniline (**1a**) the fluorescence and phosphorescence are well resolved and their quantum yields can be determined directly from the total emission spectrum. The overlapping fluorescence and phosphorescence spectra of the *N*-arylbenzamides were resolved by time dependent integration: fluorescence spectra were integrated for a period of 1 ns beginning 1 ns after the excitation pulse, whereas the phosphorescence spectra were integrated for 500 ns beginning 300 ns after the excitation pulse. Their fluorescence and phosphorescence quantum yields were calculated by comparing their intensities with those for aniline obtained under the same conditions. All emission spectra are uncorrected, and the estimated error for the quantum yields is ±20%. Fluorescence decays were measured on a Photon Technologies International (PTI) Timemaster stroboscopic detection instrument with a gated hydrogen or nitrogen lamp using a scatter solution to profile the instrument response function. Phosphorescence decays were measured on a PTI Timemaster phosphorescence-time-based detection instrument excited with a Xenon flash lamp as the excitation source. Nonlinear least-squares fitting of the decay curves employed the Levenburg−Marquardt algorithm as described by James et al.[11] and implemented by the Photon Technologies International Timemaster (version 1.2) software. Goodness of fit was determined by judging the χ^2 (<1.3 in all cases), the residuals, and the Durbin−Watson parameter (>1.6 in all cases). Solutions degassed under vacuum (<0.1 Torr) through five freeze−pump−thaw cycles have similar quantum yields and lifetimes at 77 K as solutions that were not deoxygenated. ZINDO(S)/CI calculations were performed using Cache Release 3.5. Ground-state structures were optimized with the AM1 method using MOPAC (version 94.10) programs. Orbital diagrams were calculated using Hyperchem 5.0 or a Visualizer program implemented in the MOPAC program package. The diagrams obtained by the two methods are essentially the same.

Materials. Benzoyl chloride, triethylamine, aniline, biphenylamine, 2-aminoanthracene, and iodomethane are commercially available and used as received. Anhydrous MTHF containing 200 ppm BHT (Aldrich) was distilled over soldium under a nitrogen atmosphere. 4-Aminodiphenylacteylene was prepared from 4-iodoaniline and cuprous 4-phenylacetylide by the method of Stephens et al.,[12] mp 127−128 °C (lit.[12] 128−129 °C). 4-Aminostilbene and 3-aminostilbene were obtained from reduction of 4-nitrostilbene and 3-nitrostilbene, respectively, using $SnCl_2 \cdot 2H_2O$.[13] Benzamide and benzanilide (Aldrich) were recrystallized with DMF and water (10:1) two times.

General Procedure for Preparing Secondary Amides. To a solution of amine (1−5 mmol) in dichloromethane (5−20 mL) was added 2 equiv of triethylamine, followed by 1 equiv of benzoyl chloride in dichloromethane (5−20 mL). After the mixture was stirred for 1 h, the solvent was removed using a rotary evaporator. The solid residue was washed with water and recrystallized from DMF/water (10:1). The resulting crystalline amide was washed with water and dried under vacum.

N-Benzoyl-4-aminobiphenyl (**2**): mp 233−234 °C (lit.[14] 233−234 °C); ^{1}H NMR (DMSO-d_6, 300 MHz) δ 7.34 (t, ^3J = 7.5 Hz, 1H), 7.46 (t, ^3J = 7.5 Hz, 2H), 7.51−7.64 (m, 3H), 7.68 (m, 4H), 7.90 (dm, ^3J = 8.7 Hz, 2H), 7.98 (dm, ^3J = 6.9 Hz, 2H), 10.36 (s, 1H, N−H).

N-Benzoyl-4-aminodiphenylacetylene (**3**): mp 208−209 °C; ^{1}H NMR (DMSO-d_6, 300 MHz) δ 7.40−7.45 (m, 3H), 7.56−7.65 (m, 7H), 7.88 (dm, ^3J = 9 Hz, 2H), 7.96 (dm, ^3J = 7.5 Hz, 2H), 10.46 (s, 1H, N−H); MS *m*/*e* (%) 297 ($M^{\bullet+}$, 100), 105 (100).

N-Benzoyl-2-aminophenanthrene (**4**): 3-Aminostilbene (0.7 g, 3.5 mmol) was dissolved in 100 mL of ether, 500 mL of hexane and I_2 (ca. 0.1 mg) were added, and the solution was irradiated at 300 nm in a Rayont RPR-100 photoreactor. The reaction was monitored by GC until the starting material was consumed (1−3 h). The irradiated solution was concentrated to ca. 5 mL. The 2-aminophenantharene was separated by column chromatography (1:1 hexane/ether as eluent) and directly benzoylated with benzoyl chloride and triethylamine since the amine is extremely air-sensitive. The crude benzamide was recrystallized from DMF/water (10:1) to give 0.35 g of **4** (34% overall yield): mp 223−225 °C (lit.[15] 216.5 °C); ^{1}H NMR (DMSO-d_6, 300 MHz) 7.52−7.75 (m, 5H), 7.77−7.88 (m, 2H), 7.94−8.12 (m, 4H), 8.53 (s, 1H), 8.81 (t, ^3J = 9 Hz, 2H), 10.58 (s, 1H); MS *m*/*e* (%) 298 (MH^+, 100), 105 ($PhCO^+$, 50).

N-Benzoyl-4-aminostilbene (**5**): mp 245−246 °C (lit.[16] 244−245 °C); ^{1}H NMR (DMSO-d_6, 300 MHz) δ 7.2−7.3 (m, 2H), 7.27 (d, ^3J = 7 Hz, 1H), 7.38 (t, ^3J = 7 Hz, 1H), 7.50−7.65 (m, 7H), 7.82 (d, ^3J = 8 Hz, 2H), 7.96 (d, ^3J = 7 Hz, 2H), 10.33 (s, 1H); MS *m*/*e* (%) 299 ($M^{\bullet+}$,18), 254 (18), 225 (26),-105 (100).

N-Benzoyl-2-aminoanthracene (**6**): mp 285 °C; ^{1}H NMR (DMSO-d_6, 300 MHz) δ 7.44−7.54 (m, 2H), 7.54−7.68 (m, 3H), 7.83 (d, ^3J = 9.6 Hz, 1H), 8.02−8.12 (m, 5H), 8.51 (s, 1H), 8.53 (s, 1H), 8.68 (s, 1H), 10.53 (s, 1H). MS *m*/*e* (%) 298 (MH^+,100).

Results

Absorption and Fluorescence Spectra. The *N*-arylbenzamides **1**−**6** were prepared via the reaction of benzoyl chloride with the corresponding amines **1a**−**6a** and characterized by their spectral data (see Experimental Section). The amides were recrystallized from 10:1 dimethylformamide and water. In some cases, repeated recrystallization was necessary to remove luminescent impurities. AM1 calculations indicate that all of the amides have planar geometries in which the *N*-aryl group is trans to the benzamide phenyl group with respect to rotation about the amide C−N bond.

The room-temperature absorption spectra of aniline (**1a**) and benzamide (**1b**) in methyltetrahydrofuran (MTHF) solution are shown in Figure 1. Also shown in Figure 1 are their luminescence spectra obtained at 77 K in a MTHF glass. The absorption and luminescence spectra of benzanilide (**1**) in MTHF and the luminescence emission and excitation spectra of microcrystalline **1** are shown in Figure 2. The overlapping fluorescence and phosphorescence spectra of **1** were resolved by time dependent integration (see Experimental Section). The luminescence excitation spectra for highly dilute glasses are similar in

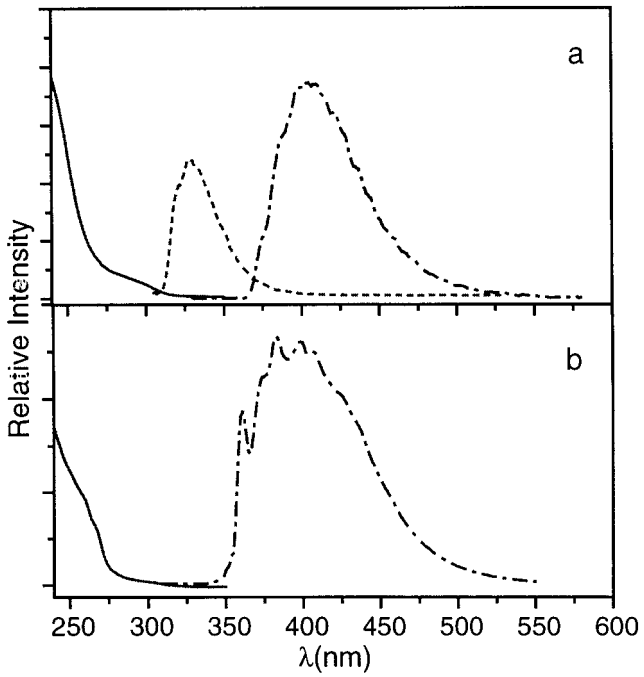

Figure 1. Absorption (solid lines) and low-temperature fluorescence (dashed lines) and phosphorescence (dash−dotted lines) spectra in MTHF: (a) aniline (**1a**, 0.14 mM); (b) benzamide (**1b**, 0.75 mM).

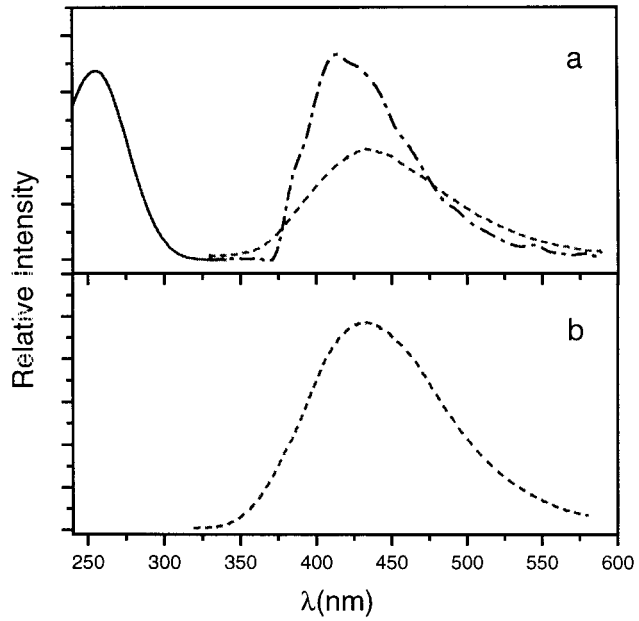

Figure 2. Absorption (solid lines) and low-temperature fluorescence (dashed lines) and phosphorescence (dash−dotted lines) spectra of benzanilide (**1**, 0.1 mM): (a) in MTHF; (b) in crystal.

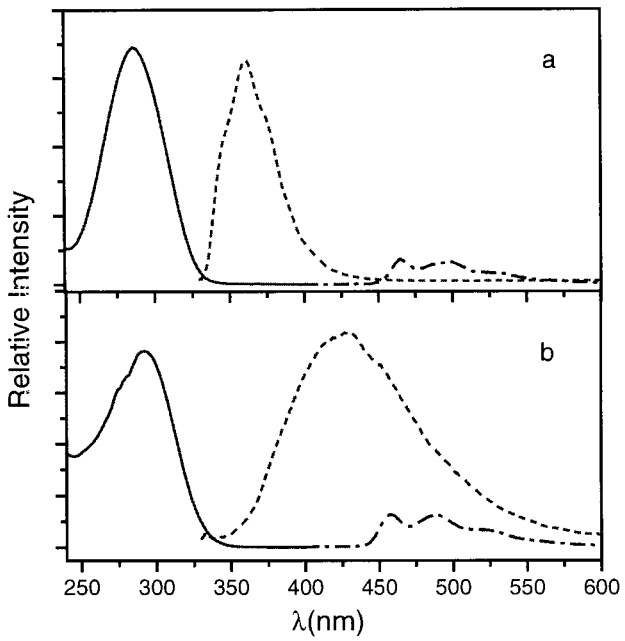

Figure 3. Absorption (solid lines) and low-temperature fluorescence (dashed lines) and phosphorescence (dash−dotted lines) spectra in MTHF: (a) biphenylamine (**2a**, 20 μM); (b) its benzamide (**2**, 15 μM).

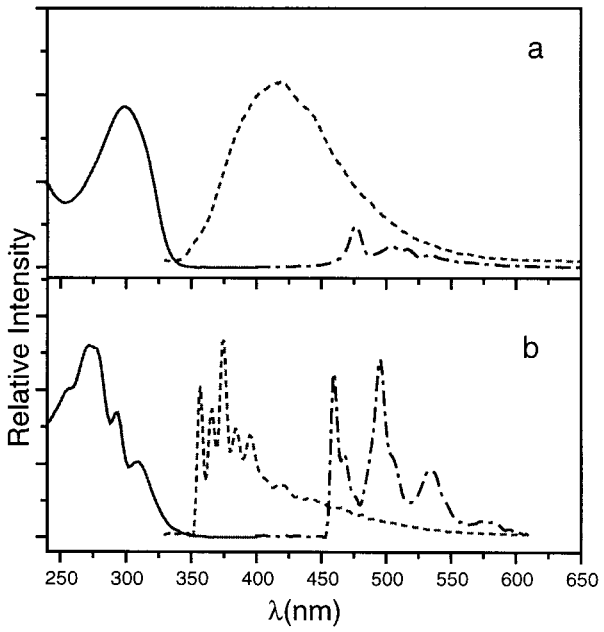

Figure 4. Absorption (solid lines) and low-temperature fluorescence (dashed lines) and phosphorescence (dash−dotted lines) spectra in MTHF: (a) benzamides of 4-aminodiphenylacetylene (**3**, 10 μM); (b) benzamide of 2-aminophenanthrene (**4**, 15 μM).

appearance to their absorption spectra. The room-temperature absorption and 77 K luminescence spectra of amine **2a** and amide **2** are shown in Figure 3 and the spectra of amides **3**−**6** are shown in Figures 4 and 5. Spectra of the amines **3a**, **5a**, and **6a** are available as Supporting Information.

Fluorescence quantum yields were determined using 9,10-diphenylanthracene ($\Phi_f = 1.0$ at 77 K in MTHF) as an external standard and phosphorescence quantum yields were estimated from the ratio of the integrated phosphorescence/fluorescence area. Weak fluorescence ($\Phi_f \sim 10^{-3}$) was detected from **1b** and no phosphorescence was detected from **5** or **6**. Single-exponential fluorescence and phosphorescence decays were obtained except in the case of the amides **4** and **6,** for which dual exponential fluorescence decay was observed. Absorption (maximum and molar absorptivity for lowest energy allowed transitions) and emission (fluorescence and phosphorescence maxima, quantum yields, and lifetimes) spectral data for amines **1a**−**6a** and amides **1b** and **1**−**6** are summarized in Table 1.

ZINDO Calculations. The electronic structure and singlet and triplet states of the amides **1**−**6** and **1b** and amines **1a**−**3a** were investigated by semiempirical INDO/S-SCF-CI (ZINDO) calculations using the algorithm developed by Zerner and co-workers.[17] Ground-state geometries were obtained from AM1 calculations. The nodal patterns for the frontier orbitals of **1a**, **1b**, **1**, and **2** are shown in Figure 6. In each case the lowest energy orbital shown is that of the amide-localized nonbonding

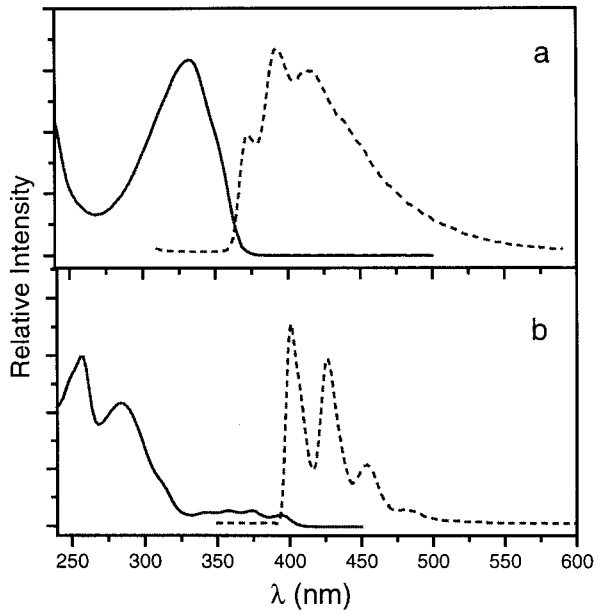

Figure 5. Absorption (solid lines) and low-temperature fluorescence (dashed lines) spectra in MTHF: (a) benzamide of 4-aminostilbene (**5**, 15 μM); (b) benzamide of 2-aminoanthracene (**6**, 12 μM).

orbital. All of the remaining frontier orbitals are π-type. In the case of amides **1** and **2** the frontier π orbitals resemble those of benzamide (**1b**) or the amines **1a** or **2a**, being localized either on the benzoyl group (B-type) or *N*-aryl group (A-type) rather than delocalized over the entire π system. Also shown in Figure 6 are the two singly occupied orbitals (SOMO) of the lowest triplet states of **1a**, **1b**, **1**, and **2**. In all cases the lower energy SOMO resembles the HOMO of the singlet ground state. The higher energy SOMO of **1a** and **1b** resemble the LUMO of the singlet; however, the higher energy SOMO of amide **1** is delocalized over both the amide and *N*-aryl groups and the SOMO of **2** resembles the SLUMO (MO53) of the singlet (Figure 6).

The calculated absorption maxima, oscillator strengths, important configurations, and character of the lowest singlet states of the amine **1a** and amides **1b** and **1**−**6** are summarized in Table 2. Data for the amines **2a**−**6a** is available as Supporting Information. The lowest energy transitions of the amines are of $\pi \rightarrow \pi^*$ character. The results of ZINDO calculations for amide **1** are similar to those we recently published using a slightly different ground-state geometry obtained from MM2 calculations.[5] The lowest excited singlet of amides **1b** and **1**−**6** is of n,B* character (carbonyl → benzoyl). The calculated energies for the n → B* transitions are all similar, and their calculated oscillator strengths are very small. The higher energy singlets of the amides can be classified as either *N*-aryl-localized (A,A*), benzoyl-localized (B,B*), or delocalized (A,B* or A,AB*) π,π^* states. The energies and oscillator strengths for the localized transitions are similar to those for the amines **1a**−**6a** (A → A* transitions) or benzamide **1b** (B → B* transition).

Discussion

Benzanilide Singlets. The absorption spectrum of amide **1** in MTHF solution consists of a single broad band with a maximum at 265 nm (Figure 2a). ZINDO calculations (Figure 6 and Table 2) suggest that three closely spaced $\pi \rightarrow \pi^*$ transitions, the strongest of which is an A,B* type (aniline → benzoyl) transition, contribute to this band. The lowest energy singlet state is predicted by ZINDO to arise from a forbidden n → B* (carbonyl → benzoyl) transition, which is not observed in the absorption or fluorescence excitation spectra, even at high concentrations. Since the energies of highly forbidden transitions are subject to computational uncertainty, it is possible that the n → B* transition is buried under the tail of the allowed $\pi \rightarrow \pi^*$ transitions, as suggested previously.[4,5]

The low-temperature luminescence of **1** was first investigated by O'Connell et al.,[7] who resolved the total luminescence into overlapping fluorescence and phosphorescence in EPA solution. The absorption and fluorescence spectral data in MTHF solution (Figure 2a and Table 1) are similar to their reported data, except for the larger luminescence quantum yields obtained in MTHF. O'Connell et al.[7] noted that the fluorescence spectrum is exceptionally broad and displays a large Stokes shift. The fluorescence maximum actually lies at a lower energy than the phosphorescence maximum (430 vs 410 nm). They suggested that the emitting singlet state differed significantly in geometry from the Franck−Condon singlet state. An even larger Stokes shift is observed for the very weak fluorescence of **1** in fluid solution and has been attributed to a TICT state formed via twisting of the amide C−N bond.[1,5,6] However, a large amplitude geometry change such as twisting about the C−N bond would seem unlikely in the glassy state. Furthermore, the fluorescence of **1** is similar in polar and nonpolar glasses and in the mircrocrystalline solid **1** (Figure 2b), suggesting that no significant charge transfer or geometry change occurs upon relaxation of the Franck−Condon state to the fluorescent state. The broad 77 K fluorescence of **1** in an EPA or MC glass has been attributed by Heldt et al.[4] to overlapping fluorescence from multiple monomer excited states and from an aggregate. However, we find that the fluorescence decay time is single exponential and invariant with emission wavelength or concentration (0.4−80 mM), suggesting a single fluorescent state.[18]

Three of the four lowest energy singlet states of **1**, as determined by ZINDO calculations (Table 2), are derived from transitions that are localized on either the aniline (A,A*) or benzoyl (n,B* and B,B*) subunits of the benzanilide molecule (Figure 6). This suggests that the spectroscopy of aniline (**1a**) and benzamide (**1b**) might provide clues as to the origin of the Stokes-shifted fluorescence of **1**. The absorption spectra of **1a** and **1b** are similar, consisting of a weak long-wavelength band and stronger shorter-wavelength band (Figure **1a**,**b**). On the basis of ZINDO calculations (Table 2) these bands are assigned to $\pi \rightarrow \pi^*$ transitions with differing extents of configuration interaction. Similar splitting of the $\pi \rightarrow \pi^*$ transitions into a weak lower energy band and a strong higher energy band is observed for monosubstituted benzenes with mesomeric substituents, including styrene.[19] ZINDO calculations indicate the presence of a low-energy-forbidden n,B* transition for **1b**, similar to that for **1**.[20]

Well-resolved fluorescence and phosphorescence are observed for **1a** at 77 K in MTHF (Figure 1a), with quantum yields and lifetimes similar to those reported by Sarkar and Kastha for a methylcyclohexane glass (Table 1).[21] The fluorescence of **1a** bears a mirror image relationship to the absorption and fluorescence excitation spectra and thus is assumed to arise from a lowest π,π^* singlet state with a geometry similar to that of the ground state.[22] Thus, it seems unlikely that relaxation of an aniline-localized A,A* state can account for the Stokes-shifted fluorescence of **1**. Heldt et al.[4] report that **1b** displays weak fluorescence at ca. 320 nm in addition to a stronger phosphorescence at 395 nm.[4] We find that the 320 nm emission present in a commercial sample of **1b** largely disappears upon recrystallization ($\Phi_f < 10^{-3}$), suggesting that it is derived from an

TABLE 1: Absorbance and Low-Temperature Emission Spectra Data for Benzamides in MTHF

		absorbance[b]		fluoresence[c]			phosphoresence[c]		
compd[a]		λ_{max} (nm)	ϵ (M^{-1})	λ_{max} (nm)	τ (ns)	QY	λ_{max} (nm)	τ (s)	QY
$PhNH_2$	**1a**	280	4400	325	1.92	0.23	405	4.42	0.45
$PhCONH_2$	**1b**	270	930	275	4.8	0.003	380	1.00	0.08
PhCONHPh	**1**	265	13600	430	2.73	0.25	410	0.40	0.37
$BpNH_2$	**2a**	286	21500	365	10.65	0.61	470	3.52	0.07
PhCONHBp	**2**	293	25400	420	3.97	0.45	460	2.00	0.07
$DpaNH_2$	**3a**	314	14900	360	1.25	0.33	480	1.57	0.02
PhCONHDpa	**3**	308	38900	430	2.06	0.44	470	0.75	0.02
PhCONHPn	**4**	309	20500	375	29.4[d]	0.13	459	4.14	0.07
$StNH_2$	**5a**	340	30100	410	1.05	0.87			
PhCONHSt	**5**	342	52200	393	1.09	0.29			
$AnNH_2$	**6a**	410	3680	480	22.60	0.94			
PhCONHAn	**6**	283	59500	401	15.1[e]	0.74			

[a] Bp = biphenyl, Dpa = diphenylacetylenyl, Pn = phenanthryl, St = stilbenyl, An = anthracenyl. [b] Measured at room temperature. [c] Measured at 77 K. [d] 4.8 ns at 450 nm. [e] Contains 30% of a second component with τ = 7.3 ns.

impurity. The absence of fluorescence from **1b** indicates that the lowest n,B* state is nonfluorescent, in agreement with its vanishingly small calculated oscillator strength (Table 2). Thus, the n,B* state of **1b** is presumed to decay via intersystem crossing or internal conversion to the ground state. The photophysical behavior of **1b** in a MTHF glass is summarized in Figure 7a.

The absence of 430 nm fluorescence from either **1a** or **1b** suggests, by a process of elimination, that both benzamide and aniline subunits are involved in formation of the fluorescent state of amide **1**. We previously suggested that barrierless torsion of the A,B* state about the C−N bond gives rise to a TICT state responsible for the 510 nm room-temperature fluorescence of **1**.[5] While such large-amplitude motion seems unlikely to occur in a glass or cyrstal, a smaller geometric change might result in the 430 nm fluorescence observed in rigid media. The nature of this change remains to be elucidated; however, preliminary exploration of the singlet-state potential energy surface indicates that a scissoring motion that compresses both the Ph−C−O and C−N−Ph dihedral angles can result in a decrease in the A,B* energy, accompanied by an increase in the ground-state energy. A repulsive potential energy surface for the ground state can help account for both the large Stokes shift and the exceptionally broad fluorescence spectrum for **1** (Figure 2a). The relaxed state, which we will refer to as S_{430}, might be reached either directly from the vertical A,B* state or via a surface crossing with the lowest n,B* state. Intersystem crossing from either the A,B* or the n,B* state can account for the observation of phosphorescence from **1**. This model for the behavior of **1** in a MTHF glass is summarized in Figure 7b.

Benzanilide Triplets. The phosphorescence spectra of aniline (**1a**) and amides **1b** and **1** are shown in Figures 1 and 2a. The spectrum of **1b** is structured, whereas those of **1a** and **1** are not structured. The lowest energy vibronic band for **1b** is at 360 nm, similar to the wavelength of the onset of emission of **1a** and **1**. The calculated center of gravity for all three bands is 405 ± 5 nm.[23] The phosphorescence decay time for **1** (0.4 s) is somewhat shorter than those for **1a** or **1b** (4.4 and 1.0 s, respectively). These decay times are typical of aromatic hydrocarbons with lowest π,π^* triplet states.[24]

The ZINDO calculations provide further support for the assignment of the phosphorescence from **1a**, **1b**, and **1** to π,π^* triplet states (Table 2). The two singly occupied orbitals of the triplets of **1a** and **1b** correspond to the HOMO and LUMO of the closed shell singlets (Figure 6). Thus, their triplets are assigned to A,A* and B,B* states, respectively (Figure 7a). In the case of **1**, the lower energy triplet-state SOMO resembles the HOMO of **1a** or **1** (*N*-aryl localized). However, the higher energy SOMO is delocalized over both rings, resembling the LUMO of a fully conjugated molecule such as stilbene. Thus, the lowest triplet of **1** is assigned an A,AB* configuration (Figure 7b). Extended conjugation should require that the triplet retain a planar geometry similar to that of the ground state, in accord with the weakly structured appearance of the phosphorescence band (Figure 2a). Similar ground-state and triplet-state potential energy surfaces can account for the overlapping fluorescence and phosphorescence spectra and the narrower phosphorescence band.

Microcrystalline Benzanilide. The luminescence excitation and emission spectra of microcrystalline **1** are shown in Figure 2b. The emission spectrum is obtained using 325 nm excitation, near the maximum in the excitation spectrum. The excitation maximum is red-shifted from that for the MTHF solution or glass due to the high optical density of the crystal. The emission band shape is similar to that in the glass (Table 1); however, the emission maximum is at somewhat shorter wavelength in the crystal (410 nm) vs glass. This may reflect a difference in molecular geometry. According to AM1 and MM2 calculations, **1** has a totally planar structure in the absence of solvent. However, in the crystal there is a moderately large 62° dihedral angle between the two phenyl groups, each group having a dihedral angle of ca. 31° with respect to the amide plane.[25]

The observation of similar luminescence for **1** in the crystal and dilute glass indicate that there is no strong electronic interaction between adjacent molecules within the crystal. Hydrogen-bonded amide molecules form one-dimensional tapes within the crystal.[25] There are no close phenyl−phenyl contacts between adjacent molecules within a tape. The close contacts between molecules in adjacent tapes are edge-to-face, which result in only weak electronic face-to-face interactions. Face-to-face π-stacking interactions are necessary for the observation of excimer fluorescence.[9]

The luminescence decay of microcrystalline **1** is dominated by a short-lived component (1.3 ns) whose decay time is somewhat shorter than that for **1** in a MTHF glass (Table 1). More rapid decay might result from a difference in molecular structure or from quenching of singlet molecules by trap sites in the interior of the crystal. In addition to short-lived fluorescence there are minor components of longer lived luminescence with maxima near 440 nm and decay times of ca. 1 μs. The longer lived emission could either be phosphorescence or delayed fluorescence.[26]

4-Aminobiphenyl and Its *N*-Arylbenzamide. The room-temperature absorption and 77 K luminescence spectra of 4-aminobiphenyl **2a**[27] and its benzamide **2** in MTHF are shown in Figure 3. The absorption spectra of **2a** and **2** display long-

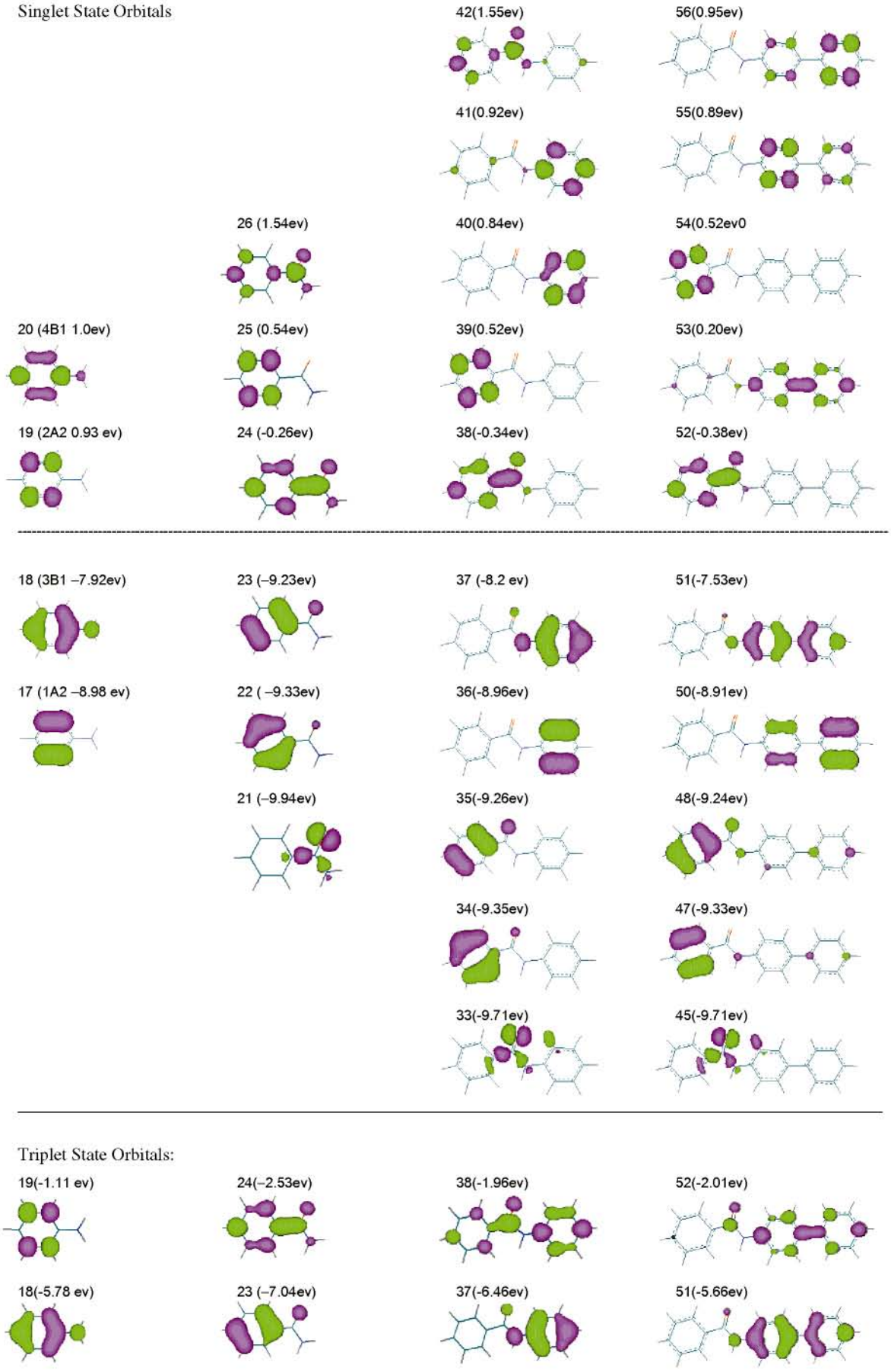

Figure 6. Diagram of frontier orbitals for **1a**, **1b**, **1**, and **2**.

TABLE 2: Excitation Wavelength, Oscillator Strength, Orbital Localization, and Composition of First Four Transitions, Calculated for Benzamides Using ZINDO/S/CI Method

compd		ΔE^a (kcal)	λ^b (nm)	f^c	TLP^d	χ^e (%)
1a	S1	101.4	282	0.0273	A,A*	$\chi_0^1(68)$, $\chi_1^1(31)$
	S2	123.3	232	0.3162	A,A*	$\chi_0^1(90)$, $\chi_1^0(8)$
	S3	142.2	202	0.041	A,A*	$\chi_0^2(91)$
	S4	147.4	194	0.7657	A,A*	$\chi_0^0(31)$, $\chi_1^1(65)$
	T1	68.0	420		A,A*	
1b	S1	82.9	345	0.0006	n,B*	$\chi_2^0(66)$, $\chi_2^2(32)$
	S2	105.1	272	0.0128	B,B*	$\chi_1^0(39)$, $\chi_0^1(28)$, $\chi_0^0(19)$, $\chi_1^1(10)$
	S3	124.3	230	0.418	B,B*	$\chi_0^0(68)$,$\chi_1^0(22)$
	S4	141.5	202	0.0027	B,B*	$\chi_3^0(57)$, $\chi_0^1(13)$, $\chi_1^0(12)$
	T1	67.9	421		B,B*	
1	S1	79.9	358	0.0002	n,B*	$\chi_4^0(70)$, $\chi_4^4(26)$
	S2	102.1	280	0.08	A,A*	$\chi_0^2(16)$,χ_0^2 (37), $\chi_1^2(22)$
	S3	103.6	276	0.37	A,B*	$\chi_0^0(67)$, $\chi_0^2(13)$
	S4	104.7	273	0.12	B,B*	$\chi_2^0(18)$,$\chi_2^1(21)$, $\chi_3^0(33)$, $\chi_3^1(10)$
	T1	68.1	420		A,A*	
2	S1	78.5	364	0.0003	n,B*	$\chi_6^0(68)$, $\chi_6^6(18)$
	S2	96.9	295	0.76	A,B*	$\chi_0^0(63)$, $\chi_0^1(13)$
	S3	97.9	292	0.09	A,A*	$\chi_0^3(39)$, $\chi_0^4(18)$
	S4	103.2	277	0.004	A,A*	$\chi_0^3(11)$, $\chi_0^4(18)$, $\chi_1^1(29)$
	T1	60.8	470		A,A*	
3	S1	79.2	361	0.0004	n,B*	$\chi_7^1(64)$, $\chi_7^6(25)$
	S2	88.5	323	1.2	A,B* + A,A*	$\chi_0^0(44)$, $\chi_0^1(42)$
	S3	96.3	297	0.02	A,A*	$\chi_0^3(50)$, $\chi_0^4(8)$
	S4	96.6	296	0.0001	A,A*	$\chi_3^0(14)$, $\chi_3^1(57)$
	T1	60.8	470		A,A*	
4	S1	79.2	361	0.0002	n,B*	$\chi_6^0(68)$, $\chi_6^5(15)$, $\chi_6^6(12)$
	S2	83.6	342	0.005	A,A*	$\chi_0^1(47)$, $\chi_1^2(32)$
	S3	95.6	299	0.42	A,B*	$\chi_0^0(57)$, $\chi_0^2(20)$
	S4	101.4	282	0.65	A,B*	$\chi_0^0(56)$, $\chi_0^2(16)$, $\chi_1^0(11)$
	T1	62.2	460		A,A*	
5	S1	78.5	364	0.0004	n,B*	$\chi_6^0(62)$, $\chi_6^6(24)$
	S2	89.9	318	1.4	A,AB*	$\chi_0^0(60)$, $\chi_0^1(30)$
	S3	95.9	298	0.02	A,A*	$\chi_0^3(47)$, $\chi_0^4(11)$
	S4	101.0	283	0.003	A,A*	$\chi_0^4(31)$, $\chi_1^4(17)$, $\chi_2^5(12)$
	T1	47.9	597		A,A*	
6	S1	78.5	364	0.0007	n,B*	$\chi_5^0(22)$, $\chi_5^1(45)$, $\chi_5^5(24)$
	S2	78.8	363	0.03	A,AB*	$\chi_0^1(12)$, $\chi_0^1(31)$, $\chi_1^0(26)$,
	S3	82.6	346	0.17	A,A*	$\chi_0^0(79)$
	S4	94.4	303	0.66	A,B*	$\chi_0^1(59)$, $\chi_1^0(20)$
	T1	37.5	762		A,A*	

[a] Transition-state energy relative to ground state (kcal/mol). [b] State energy in wavelength. [c] Oscillator strength. [d] Transition localization property: A = π orbital localized on arylamine moiety, B = π orbital localized on benzoyl moiety, n = n orbital localized on CO moiety, AB = delocalized π orbital. [e] Percentage of transitions: χ_m^n symbolizes a transition from a (HOMO + m) orbital to (LUMO + n) orbital.

wavelength bands with maxima at 286 and 292 nm, respectively. These bands are assigned, based on ZINDO calculations, to allowed $\pi \rightarrow \pi^*$ transitions: of A,A* and A,B* character for **2a** and **2**, respectively. Weaker transitions at lower energy are predicted for both **2a** and **2**, the former of A,A* character and the latter of n,B* character. The calculated energy and oscillator strength for the n,B* state of **2** are similar to those for **1**.

The luminescence spectrum of **2a** displays weakly structured fluorescence with a maximum at 365 nm and structured phosphorescence with a highest energy vibronic band at 425 nm. The fluorescence and phosphorescence of **2a** are similar in appearance to those of unsubstituted biphenyl and are assigned to the lowest energy A,A* singlet and triplet states, respectively. The time-resolved luminescence spectra of **2** consists of a broad fluorescence band at 430 nm and a structured phosphorescence band with a highest energy maximum at 460 nm. The fluorescence band is similar in band shape and decay time to the fluorescence of amide **1** (Table 1) and thus is assigned to the relaxed S_{430} singlet state. The phosphorescence band is similar in band shape and decay time to the phosphorescence of amine **2a** and thus is assigned to an amine-localized A,A* triplet state, an assignment supported by the ZINDO calculation (Table 2). The state-energy diagram for amide **2** is similar to that of amide **1** (Figure 7b) except that the lowest triplet is of A,A* character.

4-Aminodiphenylacetylene and Its Benzamide. The absorption spectra of **3a** (not shown) and **3** (Figure 4a) display broad long-wavelength absorption bands with maxima at 314 and 310 nm, respectively. These bands are assigned on the basis of ZINDO calculations to allowed $\pi \rightarrow \pi^*$ transitions having A,A* and A,B* character for **3a** and **3**, respectively. As in the case of **1** and **2**, the ZINDO calculations predict the presence of a forbidden n $\rightarrow$ B* transition at a lower energy than the A $\rightarrow$ B* transition of **3** (Table 2). The fluorescence spectrum of **3** (Figure 4a) is similar in appearance and decay time to those of **1** and **2** and is assigned to the relaxed S_{430} state. The phosphorescence of **3** has the same structured appearance and a decay time similar to that of the amine **3a** and thus is assigned to a A,A* triplet state. Thus, the state-energy diagram for **3** is identical to that for **1** and **2** (Figure 7b).

2-Aminophenanthrene and Its Benzamide. 2-Aminophenanthrene **4a** was not isolated due to its sensitivity toward air oxidation and was converted directly to the amide **4**. The absorption spectrum of **4** (Figure 4b) displays a maximum at 309 nm and shoulders at lower energy. The appearance of the absorption spectrum is similar to that of phenanthrene, but broadened. According to the ZINDO calculation (Table 2), the maximum can be assigned to an allowed A $\rightarrow$ B* transition predicted to occur at 299 nm and the shoulders to an A $\rightarrow$ A* transition predicted to occur at 342 nm. As is the case for amides **1**−**3**, a forbidden n $\rightarrow$ B* transition is predicted to lie below these $\pi \rightarrow \pi^*$ transitions.

The luminescence spectrum of **4** (Figure 4b) consists of a structured fluorescence band with a long-wavelength tail and a structured phosphorescence band. The structured fluorescence and phosphorescence bands are similar in appearance to those of the unsubstituted phenanthrene.[24] The fluorescence decay of **4** determined at 375 nm is dual exponential, the major and minor components having decay times or 29.4 and 4.8 ns. The decay determined at 450 nm is monoexponential with a decay time of 4.8 ns, similar to that of the S_{430} singlets of amides **1**−**3**. Thus, the fluorescence of **4** apparently consists of two overlapping bands: a structured shorter-wavelength emission assigned to a phenanthrene-localized A,A* singlet and the broad long-wavelength emission assigned to a relaxed S_{430} state. The structured phosphorescence is assigned to an A,A* triplet and its decay time is 4.1 s, similar to that of phenanthrene in an EPA glass (3.4 s).[24]

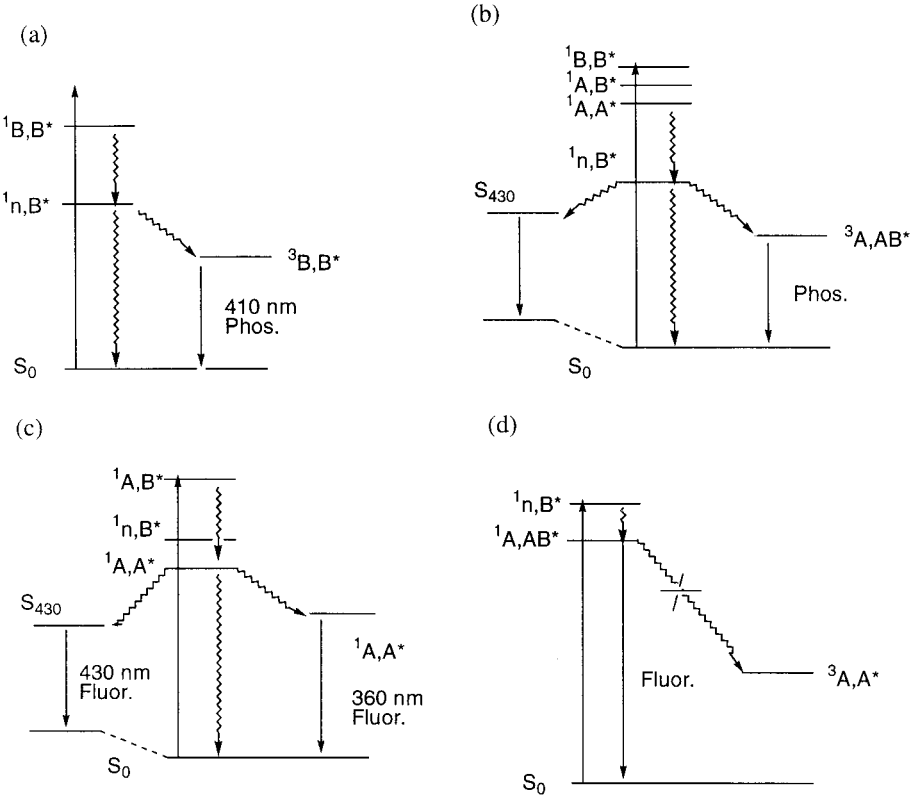

Figure 7. Proposed state-energy diagrams for (a) **1b**, (b) **1**−**3**, (c) **4**, and (d) **5** and **6**.

The occurrence of dual fluorescence for amide **4** can be explained using the state-energy diagram in Figure 7c. Excitation of one of the allowed $\pi \rightarrow \pi^*$ transitions followed by internal conversion can yield either the A,A* state or the relaxed S_{430} state. Even though the A,A * state is of higher energy than the S_{430} state, the only likely pathway from the former to the latter state would be via the planar n,B* state. Since the center of gravity of the A,A* fluorescence lies below the calculated energy of the planar n,B* state, the two singlets decay independently. It would be interesting to determine which of these singlet states is responsible for formation of the A,A* triplet; however, a method for investigating this question is not readily apparent.

4-Aminostilbene and Its Benzamide. The absorption spectra of both 4-aminostilbene (**5a**, not shown) and its benzamide **5** (Figure 5a) have a single broad long-wavelength band. The absorption maximum of **5a** is at 316 nm in hexane solution and is attributed by ZINDO to an allowed, predominantly HO → LU, $\pi \rightarrow \pi^*$ transition.[28] The absorption maximum of **5** lies at 342 nm, the only case in which a significant red shift is seen for the amide vs amine (Table 1). This absorption band is attributed by ZINDO predominantly to an allowed, A → AB*, HO → LU transition in which the HO is localized on stilbene, but the LU is delocalized over the entire molecule (Table 2). Increased delocalization presumably is responsible for the red shift in the absorption band in comparison to the amine **5a**. As is the case for amides **1**−**4**, a forbidden n → B* transition is predicted to lie below the $\pi \rightarrow \pi^*$ transitions.

The fluorescence spectrum of amide **5** (Figure 5a) resembles that of amine **5a** but, like the absorption spectrum, is red-shifted (from 380 nm for **5a** to 393 nm for **5** in a MTHF glass). The fluorescence decay times for **5a** and **5** are 1.1 and 1.7 ns, respectively. Thus, the structured fluorescence of **5** is assigned to a delocalized A,AB* singlet state. The fluorescence spectrum of **5** possesses a long-wavelength tail that is not observed for the amine **5a**. However, the fluorescence decay time remains constant and single exponential across the entire fluorescence band. Since this decay time is shorter than that for the S_{430} state of **1**−**3**, we conclude there is only one emitting singlet state. This raises the question as to why emission is observed from the stilbene-localized A,AB* state rather than the lower energy S_{430} state? The 0,0 energy of the A,AB*, estimated from the crossing point of the absorption and fluorescence spectra (Figure 5), is 365 nm. This is similar to the calculated singlet n,B* energy (Table 2), which is subject to computational uncertainty. Thus, the vertical A,AB* singlet may be of lower energy than the vertical n,B* singlet. If the latter is not populated by internal conversion from a higher energy spectroscopic singlet state, then relaxation to form the S_{430} state cannot occur. This situation is shown schematically in Figure 7d.

No phosphorescence is detected for either the amine **5a** or the amide **5**. Unsubstituted *trans*-stilbene and many of its derivatives are also nonphosphorescent in low-temperature glasses.[29] This results from a combination of factors: a short singlet lifetime, slow intersystem crossing due to the large singlet−triplet energy gap, and rapid nonradiative decay of the triplet due to its conformational flexibility. The intersystem crossing rate constant for stilbene is estimated to be ca. 4×10^7 s^{-1}. Assuming a similar rate constant for intersystem crossing of **5**, its quantum yield for intersystem crossing would be ca. 0.05. The large singlet−triplet energy gap and absence of intersystem crossing in **5** is indicated in Figure 7d.

2-Aminoanthracene and Its Benzamide. The absorption spectra of both 2-aminoanthracene **6a**[30] (not shown) and the amide **6** (Figure 5b) display a weak long-wavelength band with a maximum near 395 nm and a strong band near 260 nm; however, the 395 band is stronger and broader for the amine. The amide has an additional band at 293 nm. On the basis of ZINDO calculations (Table 2) the 395 nm band of **6** can be assigned to an A → AB* delocalized transition similar to that

for **5**. The low-temperature luminescence spectra of **6a** and **6** consist of structured fluorescence with a highest energy maximum at 470 nm for **6a** and 405 nm for **6**. Both the absorption and fluorescence of **6** are blue-shifted with respect to those of **6a**. The absence of S_{430} fluorescence from **6** is consistent with a lower energy for the Franck−Condon A,AB* vs n,B* state, as in the case of **5** (Figure 7d).

The fluorescence decay of **6** is dual exponential, with decay times of 15.1 and 7.3 ns. Neither the decay times nor the preexponentials are dependent upon the emission wavelength. The two decays are tentatively assigned to the syn and anti rotamers with respect to the *N*-anthracene bond, both of which retain trans configurations with respect to the amide C−N bond.

The syn and anti rotamers of some 2-vinylanthracenes are known to have similar spectra but display different photophysical behavior.[31] The observation of emission from two rotamers of **6** but not from amides **1**−**5** most likely reflects the presence of an axis of symmetry (or quasi-axis) for *N*-aryl rotation in amines **1a**−**5a**.

No phosphorescence is observed in a MTHF glass for either amine **6a** or amide **6**. The absence of phosphorescence no doubt reflects very slow intersystem crossing resulting from a large singlet−triplet gap (Figure 7d). Anthracene derivatives display phosphorescence only when the second triplet lies beneath the lowest singlet.[24]

Concluding Remarks. The photophysical behavior of the six *N*-arylbenzamides is highly dependent upon the electronic interactions between benzamide and aminoarene portions of the molecules. Assignment of the absorption, fluorescence, and phosphoresce spectra of these amides has made use of comparisons with the spectra of benzamide and the aminoarenes and with semiempirical ZINDO calculations. For all of the amides the lowest energy bands in the absorption spectra can be assigned to $\pi \rightarrow \pi^*$ transitions that are either arene-localized (A → A*) or of arene → amide character (A → B* or A → AB*). In the case of **1**−**4** the amines and amides have similar singlet energies; however, the singlet energy of **5** is lower than that of **5a**, whereas the energy of **6** is higher than that of **6a**.

Amides **1**−**3** display broad Stokes-shifted emission with a maximum at 430 nm, rather than the higher energy structured emission expected from the lowest π,π^* singlet states. This anomalous Stokes-shifted fluorescence is attributed to a singlet state, S_{430}, formed upon relaxation of a π,π^* or n,B* state, which is of lower energy than the lowest π,π^* singlet states. The n,B* state is not observed spectroscopically but is predicted by ZINDO calculations to lie at 360 nm for benzamide and all six *N*-arylbenzamides. The amides **5** and **6** have lowest energy π,π^* states and thus show structured emission at a higher energy than the S_{430} emission. The phenanthrene carboxamide **4** shows dual fluorescence from both π,π^* and S_{430} singlet states. The absence of fluorescence from benzamide is attributed to rapid intersystem crossing from a lowest n,B* singlet to the π,π^* triplet. Amides **1**−**4** display structured phosphorescence assigned to delocalized π,π^* delocalized triplet states. No phosphorescence is observed for amides **5** and **6**. Inefficient intersystem crossing results primarily from the large singlet−triplet splitting for these amides.

The results of this investigation are of relevance to the ongoing controversy surrounding the Stokes-shifted room-temperature fluorescence of benzanilide in nonpolar solvents.[2−5] The nonspectroscopic vertical n,B* state is expected to lie below the π,π^* singlet states in solution as well as in low-temperature glasses. A larger amplitude geometry change in solution vs the glass could account for the larger Stokes shift observed in solution. Extended conjugation of the *N*-aryl subunit might also invert the ordering of n,B* and π,π^* states in solution. The spectroscopy of secondary and tertiary *N*-arylbenzamides in solution and the solid state is the subject of continuing investigation.

Acknowledgment. We thank Prof. Siegfried Schneider for helpful discussions. Financial support for this research has been provided by the National Science Foundation.

Supporting Information Available: Absorption and low-temperature fluorescence and phosphorescence spectra for *N*-arylamines **3a**, **5a**, and **6a** in MTHF. Excitation wavelength, oscillator strength, and composition of first four transitions calculated for *N*-arylamines (**2a**, **3a**, **5a**, **6a**) using ZINDO/S/CI method. This information is available free of charge via the Internet at http://pubs.acs.org.

References and Notes

(1) (a) Tang, G.-Q.; MacInnis, J.; Kasha, M. *J. Am. Chem. Soc.* **1987**, *109*, 2531. (b) Heldt, J.; Gormin, D.; Kasha, M. *Chem. Phys. Lett.* **1988**, *150*, 433. (c) Heldt, J.; Gormin, D.; Kasha, M. *J. Am. Chem. Soc.* **1988**, *110*, 8255. (d) Heldt, J.; Gormin, D.; Kasha, M. *Chem. Phys.* **1989**, *136*, 321.

(2) Lucht, S.; Stumpe, J.; Rutloh, M. *J. Fluorescence* **1998**, *8*, 153.

(3) Azumaya, I.; Kagechika, H.; Fujiwara, Y.; Itoh, A.; Yamaguchi, K.; Shudo, K. *J. Am. Chem. Soc.* **1991**, *113*, 2833.

(4) Heldt, J.; Heldt, J. R.; Szatan, E. *J. Photochem. Photobiol. A.* **1999**, *121*, 91.

(5) Lewis, F. D.; Long, T. M. *J. Phys. Chem. A* **1999**, *102*, 5327.

(6) The Stokes-shifted solution fluorescence was initially attributed to Kasha and co-workers[1] to an imidol tautomer formed via a double proton transfer in a hydrogen-bonded dimer. This assignment has been adopted in some more recent publications.[2,4] Evidence against imidol formation has been presented by Azumaya et al.[3] and by Lewis and Long.[5]

(7) O'Connell, E. J., Jr.; Delmauro, M.; Irwin, J. *J. Photochem. Photobiol.* **1971**, *14*, 189.

(8) (a) Lewis, F. D.; Barancyk, S. V.; Burch, E. L. *J. Phys. Chem.* **1992**, *96*, 4, 3866. (b) Lewis, F. D.; Burch, E. L. *J. Phys. Chem.* **1996**, *100*, 4055.

(9) Lewis, F. D.; Yang, J.-S. *J. Phys. Chem.* **1997**, *101*, 1775.

(10) Li, R.; Lim, E. C. *J. Chem. Phys.* **1972**, *57*, 605.

(11) James, D. R.; Siemiarczuk, A.; Ware, W. R. *Rev. Sci. Instrum.* **1992**, *63*, 1710.

(12) Stephens, R. D.; Castro, C. E. *J. Org. Chem.* **1963**, *28*, 3313.

(13) Bellamy, F. D.; Ou, K. *Tetrahedron Lett.* **1984**, 839.

(14) Shine, H. J.; Cheng, J. D. *J. Org. Chem.* **1971**, *36*, 2787.

(15) Kunz, J. *Justus Liebigs Ann. Chem.* **1902**, *321*, 319.

(16) Pfeiffer, P.; Sergiewskaja, S. *Chem. Ber.* **1911**, *44*, 1112.

(17) (a) Bacon, A. D.; Zerner, M. C. *Theor. Chim. Acta* **1970**, *53*, 21. (b) Zerner, M. C.; Loew, G. H.; Kircher, R. R.; Mueller-Westerhoff, U. T. *J. Am. Chem. Soc.* **1980**, *102*, 589.

(18) The weak 320 nm emission observed by Heldt et al.[4] in low-temperature glasses was not observed by O'Connell et al.[7] or in the present investigation. We suspect that it arises from aniline, present as an impurity or formed as a photoproduct of **1a**.[2,3]

(19) Lewis, F. D.; Bassani, D. M.; Caldwell, R. A.; Unett, D. J. *J. Am. Chem. Soc.* **1994**, *116*, 10477.

(20) The lower energy band of **1b** has been assigned by Heldt to an n → π^* transition.[4]

(21) Sarkar, S. K.; Kastha, G. S. *Spectrochim. Acta* **1992**, *48A*, 1611.

(22) Aniline is pyramidally distorted at the NH_2 group in the ground state but quasi-planar in the lowest singlet state: Sinclair, W. E.; Pratt, D. W. *J. Chem. Phys.* **1996**, *105*, 7942.

(23) Berlman, I. B. *Handbook of Fluorescence Spectra of Aromatic Molecules*, 2nd ed.; Academic Press: New York, 1971; p 27.

(24) Birks, J. B. *Photophysics or Aromatic Molecules*; Wiley-Interscience: London, 1970; p 193.

(25) Kashino, S.; Ito, K.; Haisa, M. *Bull. Chem. Soc. Jpn.* **1979**, *52*, 365.

(26) Birks, J. B. *Photophysics or Aromatic Molecules*; Wiley-Interscience: London, 1970; p 523.

(27) Hashimoto, S.; Thomas, J. K. *J. Phys. Chem.* **1984**, *88*, 4044.

(28) Lewis, F. D.; Kalgutkar, R. Unpublished results.

(29) Görner, H.; Schulte-Frohlinde, D. *J. Phys. Chem.* **1979**, *83*, 3107.

(30) Rosenberg, H. M.; Eimutis, L. E. *Spectrochim. Acta* **1966**, *22*, 1751.

(31) Mazzucato, U.; Momicchioli, F. *Chem. Rev.* **1991**, *91*, 1679.